Available online at www.eccomasproceedia.org
Eccomas Proceedia COMPDYN (2017) 4224-4233

ECCOMAS
Proceedia

6th ECCOMAS Thematic Conference on
Computational Methods in Structural Dynamics and Earthquake Engineering
M. Papadrakakis, M. Fragiadakis (eds.)
Rhodes Island, Greece, 15–17 June 2017

COMPARING EN1998-3 AND KAN.EPE. MODELS FOR RETROFITTING REINFORCED CONCRETE COLUMNS WITH INADEQUATE DUCTILITY

Nefeli V. Peponi[1], Stephanos E. Dritsos[2], and Sotiria N. Athanasopoulou[3]

[1] Civil Engineer
Department of Civil Engineering, University of Patras, Greece
e-mail: nef_pep@yahoo.gr

[2] Professor
Department of Civil Engineering, University of Patras, Greece
email: dritsos@upatras.gr

[3] Civil Engineer
Department of Civil Engineering, University of Patras, Greece
email: sotiria90@gmail.com

Keywords: Column, EC8-3, KAN.EPE, Fiber Reinforced Polymers, Ductility, Reinforcement Corrosion.

Abstract. *Many existing structures which are designed according to older anti-seismic regulations appear to have insufficient seismic behavior. One of the most critical factors that contributes to the vulnerability of those structures is either insufficient ductility or significant corrosion of the reinforcement. This article investigates through experimental results the use of composite materials (fiber reinforced polymers) for strengthening columns of reinforced concrete with corroded and non-corroded reinforcement and the influence of the strengthening on the local ductility of the elements. Then, a presentation and comparison between the two available regulations of KAN.EPE. and Eurocode 8, part 3 is performed as far as the strengthening of linear elements to increase their ductility is concerned. In a second phase, a comparison between the resulting ductility of experimental results and the results of the above two regulations is carried out in order to highlight any ambiguities in the regulations.*

Peer-review under responsibility of the organizing committee of COMPDYN 2017.
doi: 10.7712/120117.5718.17710

1 INTRODUCTION

Many existing reinforced concrete structures have been designed and constructed according to old regulations or even in the absence of regulations. As a consequence, they suffer from reduced seismic capacity. One of the most critical factors that contribute to the seismic vulnerability of these structures is inadequate ductility, i.e. an insufficient capacity of the elements to develop residual deformations after reaching their maximum strength resulting in sudden brittle failure. In addition, many of these structures have developed significant corrosion in their reinforcement because of their age or due to the extremely close placement of the transverse reinforcement to the outer surface of the concrete. Notably, the rusting problem is intensified by the widespread use of S500 steel, which is more susceptible to corrosion.

The increase in local ductility of linear elements can be achieved by imposing external confinement (in the form of collars, jackets or external connectors), or by the application of a reinforced concrete jacket. The material which is most extensively used for external confinement is either steel or composite materials (fiber reinforced polymers (FRP)). Confronting the vulnerability of corroded elements can also be carried out by the assistance of external confinement, with the most common method of confinement being that of FRPs. This article investigates the strengthening of damaged reinforced concrete columns with materials and detailing emulating older construction, insufficient ductility, and reinforcement corrosion using FRP jackets.

Both the Greek Code of Structural Interventions, (KAN.EPE.) [1] and Eurocode 8, part 3 (EC8-3) [2] propose models to determine the local ductility of reinforced concrete columns unstrengthened or strengthened using composite layers. Moreover, models of experimental data have emerged as an alternative procedure to that proposed by EC8-3 [2] according to researchers such as Fardis [3]. This article extensively presents these models, which are then applied to experimental data, compared with each other and evaluated. Finally, ambiguities and weaknesses in the relationships of the above models are clarified.

2 SIMULATION MODELS OF INTERVENTION AIMED AT INCREASING LOCAL DUCTILITY

The calculation of the local ductility of linear elements unstrengthened or strengthened with FRPs is determined in terms of chord rotation, μ_θ. Approximate formulas are presented in KAN.EPE. [1], analytical types are included in EC8-3 [2] and alternative methods according to Fardis [3] can be used to calculate the curvature ductility index. These models are presented in detail below.

2.1 KAN.EPE model

According to KAN.EPE. [1], the total displacement ductility index equals the chord rotation ductility index ($\mu_\delta = \mu_\theta$). The total displacement ductility index can be calculated from one of the following equations:

$$\mu_\delta = \mu_\theta = \frac{\mu_\varphi + 2}{3} \tag{1}$$

$$\mu_\delta = \mu_\theta = \frac{\mu_\varphi + 1}{2} \tag{2}$$

where μ_φ is the curvature ductility index, which can be approximately determined from:

$$\mu_\varphi = \frac{\varepsilon_{cu,c}}{2.2\ \varepsilon_{sy} v} \tag{3}$$

where $\varepsilon_{cu,c}$ is the reduced deflection of the concrete, which is given by the equations:

$$\varepsilon_{cu,c} = 0.004 + 0.4\frac{\alpha\,\rho_{sx}\,f_{yw}}{f_{cc}} \quad (4)$$

for unstrengthened columns, or

$$\varepsilon_{cu,c} = \gamma_{IOII}\,0.0035(f_{cc}/f_c)^2 \quad (5)$$

for strengthened columns. ε_{sy} is the average yield deformation of the longitudinal reinforcement of the element, υ is the normalized axial force (positive for compression), α is the confinement efficiency index, $\rho_{sx}=\frac{A_{sx}}{b_w s_h}$ is the percentage of the transverse reinforcement parallel to the direction x of the loading, f_{yw} is the average yield strength of the stirrups, f_{cc} can be determined from:

$$f_{cc} = f_c\left(1 + 3.5\left(\frac{a_f\,\rho_f\,f_u}{f_c}\right)^{\frac{3}{4}}\right) \quad (6)$$

γ_{IOII} = 1.0 or 2.0 for carbon fiber reinforced polymer (CFRP) or glass fiber reinforced polymer (GFRP), respectively, f_c is the concrete compressive strength, A_{sx} is the area of the steel, b_w is the section width, s_h is the stirrup spacing, a_f is the confinement effectiveness index of the CFRP or the GFRP, $\rho_f=\frac{2t_f}{b_w}$ is the percentage of FRP parallel to the direction of the load, f_u is the ultimate strength of the stirrups, and t_f is the nominal thickness of the FRP.

2.2 Eurocode model

The rotation chord ductility index is the ratio of the limit value of total capacity of the chord rotation (θ_u) to the chord rotation of the element at yielding (θ_y), i.e. $\mu_\theta = \theta_u/\theta_y$. The limit value of the total chord rotation capacity of a non-confined element can be calculated from the following equation:

$$\theta_{um} = 0.0016(0.3^{\nu})\left[\frac{\max(0{,}01;\omega')}{\max(0{,}01;\omega)}f_c\right]^{0{,}225}\min\left(9;\frac{L_v}{h}\right)^{0{,}35}25^{(\alpha_s\rho_{sx}\frac{f_{yw}}{f_c})}(1.25^{100\rho_d}) \quad (7)$$

where ω and ω' are the mechanical reinforcement ratio and the compressive longitudinal reinforcement ratio, respectively, L_v is the ratio of the moment to the shear strength in the outer section, h the height of the section, ρ_d is the diagonal reinforcement ratio, and α_s is a transverse reinforcement confinement effectiveness factor, which can be calculated from the following equation:

$$\alpha_s = 1 - \frac{b_o^2 + h_o^2}{3b_o h_o} \quad (8)$$

where b_o and h_o are the dimensions of the concrete core based on the axes of the longitudinal reinforcement.

The total capacity of the chord rotation of the section confined with FRPs can be calculated from the following relationship:

$$\theta_{um} = 0.0016\cdot(0.3^{\nu})\left[\frac{\max(0.01;\omega')}{\max(0.01;\omega)}f_c\right]^{0{,}225}\min\left(9;\frac{L_v}{h}\right)^{0.35}25^{(\alpha_s\rho_{sx}\frac{f_{yw}}{f_c}+\,a_f\rho_f\frac{f_{f,e}}{f_c})}(1.25^{100\rho_d}) \quad (9)$$

where α_f is the confinement efficiency index of the FRP which can be calculated from the relationship:

$$\alpha_f = 1 - \frac{(b-2R)^2 + (h-2R)^2}{3bh} \quad (10)$$

where b and h are the full dimensions of the cross section, R is the radius of the rounded corners of the section, $\rho_f = 2t_f/b$ is the ratio of FRP parallel to the direction of the loading, $f_{f,e}$ is

the active stress of the material retrofitting the section and is given by the following relationship:

$$f_{f,e} = \min(f_{uf}, \varepsilon_{uf}, E_f)\,(1 - 0.7\,\min(f_{uf}, \varepsilon_{uf}, E_f)\frac{\rho_f}{f_c}) \quad (11)$$

where f_{uf} and E_f are the strength and modulus of elasticity of the FRP, respectively, and ε_{uf} is a marginally reduced deflection which, when not given a different value, can be taken as 0.015 for CFRP and 0.02 for GFRP.

The product $a_f \rho_f \frac{f_{f,e}}{f_c}$ from equation (9) can also be written as:

$$a_f \rho_f \frac{f_{f,e}}{f_c} = a_f \frac{\omega_w}{2}(1 - 0.35\,\omega_w) \quad (12)$$

where $\omega_w = \frac{4\,t_f\,f_u}{b f_c}$ is the volumetric confinement rate for a square section.

The chord rotation at yielding is determined by the following relationship:

$$\theta_y = \varphi_y \frac{L_V + a_v z}{3} + 0.0014\left(1 + 1.5\frac{h}{L_v}\right) + 0.125\varphi_y \frac{d_{bL} f_y}{\sqrt{f_c}} \quad (13)$$

where, φ_y is the curvature of the cross section at yielding, $a_v z$ is a term which expresses the influence of the "displacement length" of the bending moment, with $\alpha_v = 1$ if the shear cracking capacity, V_{R1}, is less than the shear force $V_{Mu} = M_y/L_v$, or else it equals 0, z is the length of the internal lever arm, which is equal to $d' - d$ in columns, d_{bL} is the diameter of the longitudinal reinforcement**,** f_y the average yield strength of the stirrups, My is the moment at yeild, d' is the depth to the compression reinforcement, and d is the effective depth of the section.

2.3 Alternative Eurocode model

According to Fardis [3], the final rotation at failure for non-retrofitted elements with a rectangular compression zone and reinforcement detailing for earthquake resistance (including the use of reinforcing bars with ribs) can be calculated from the following relationship:

$$\theta_u = \alpha_{st}(1 - 0.43\alpha_{cy})\left(1 + \frac{a_{sl}}{2}\right)(1 - 0.4\alpha_{w,r})\left(1 - \frac{2}{7}\alpha_{w,nr}\right)(0.3^{\nu})\left[\frac{\max(0.01;\omega')}{\max(0.01;\omega)} f_c\right] 0.225[\min(9; \frac{L_v}{h})]$$
$$0.35\,25^{\alpha\,\rho_s \frac{f_{yw}}{f_c}}\,(1.25^{100\rho_d}) \quad (14)$$

where $\alpha_{st} = 0.0185$ for hot rolled steel and 0.0115 for cold rolled steel, $\alpha_{cy} = 0$ for monotonic loading and $\alpha_{cy} = 1$ for cyclic loading, $\alpha_{sl} = 1$ if there is slippage in the longitudinal reinforcement and 0 if not, $\alpha_{w,r} = 1$ for rectangular walls, otherwise $\alpha_{w,r} = 0$, and $\alpha_{w,nr} = 1$ for T, H or U shaped section walls or hollow rectangular sections, otherwise it equals 0.

For columns confined with FRP, the target chord rotation at failure is determined by the above type of equation with the exponent of the term 25 increased by the factor $a_f \rho_f \frac{f_u}{f_c}$, which addresses the confinement material, as follows:

$$\theta_u = \alpha_{st}\,(1 - 0.43\alpha_{cy})\left(1 + \frac{a_{sl}}{2}\right)(1 - 0.4\,\alpha_{w,r})\left(1 - \frac{2}{7}\alpha_{w,nr}\right)(0.3\nu)\left[\frac{\max(0.01;\,\omega_2)}{\max(0.01;\,\omega_1)} f_c\right] 0.225[\min(9;$$
$$\frac{L_v}{h})] 0.35\,25^{\alpha\,\rho_s \frac{f_{yw}}{f_c} + a_f \rho_f \frac{f_u}{f_c}}\,(1.25^{100\rho_d}) \quad (15)$$

The term $a_f \rho_f \frac{f_u}{f_c}$ can be estimated by noting that:

$$f_u = f_{fe} = \min(f_{u,nom};\, \varepsilon_{uf} E_f)\,(1 - \min[\,0.5;\, 0.7\,\min(f_{u,nom};\, \varepsilon_{uf} E_f)\,\frac{\rho_f}{f_c}) \quad (16)$$

where $f_{u,nom}$ is the nominal capacity of the strengthening material, or by using one of the following equations:

$$(a_f \rho_f \frac{f_u}{f_c}) = \alpha_f \min[1.0; \min(f_{u,nom}; \varepsilon_{ufl} E_f) \frac{\rho_f}{f_c}) (1 - 0.4 \min[1.0; \min(f_{u,nom}; \varepsilon_{ufl} E_f) \frac{\rho_f}{f_c}]) \quad (17)$$

where $\varepsilon_{ufl} = 0.015$, or

$$(a_f \rho_f \frac{f_u}{f_c}) = a_f c_f \min[0.4; \frac{\rho_f f_{uf,L\&T}}{f_c}] (1 - 0.5\min [0.4; \frac{\rho_f f_{uf,L\&T}}{f_c}]) \quad (18)$$

where $f_{uf,L\&T} = E_f \varepsilon_{uf2}$, with ε_{uf2} approximately equal to 60% of the nominal value of the deformation failure, and $c_f = 1.80$ for CFRP or 0.80 for GFRP.

3 RESULTS AND COMPARISONS

For the comparison of the aforementioned models amongst themselves and with actual data, the results from a previous experimental study were used. The experimental study was conducted by Bousias et al. [4], where 6 reinforced concrete specimens were constructed and tested in their strong direction. Those specimens had the same steel reinforcement and detailing as structures constructed before 1980 and the steel reinforcement was corroded. In other words, the experimental study concerned simulating non-seismically designed and reinforced elements exposed to cyclic loading. The force-displacement diagrams of the specimens were idealized as bilinear and, thereby, the values of shear force and displacement of the tested specimens were determined at yield and failure. With the data obtained, the experimental ductility index, μ_δ, could be easily calculated.

3.1 Experimental data

The columns investigated were the half of the height of a standard floor height (1.60 m) with rectangular dimensions of 250x500 mm as shown in figure 1. The longitudinal reinforcement was 4Φ18 ribbed bars while the transverse steel was smooth bars of Φ8/200 mm. Ready-mixed concrete class C12/15 was used for the specimens. The longitudinal reinforcement had a yield stress of 595.5 MPa. For every column, a 50 mm radius of the rounded corner of the section and a 20 mm concrete cover were assumed. The materials used for the strengthened specimens were either 2 layers of CFRP with $t_f = 0.13$ mm, $E_f = 230$ GPa, $f_u = 3450$ Mpa and $\varepsilon_{ju} = 0.015$ or 5 layers of CFRP with $t_f = 0.17$ mm, $E_f = 70$ GPa, $f_u = 2170$ MPa and $\varepsilon_{ju} = 0.031$. The reinforcement of the columns were considered to be hot rolled and continuous without lap splices. Finally, the ratio L/h of columns was 3.2. Table 1 lists the characteristics of the columns.

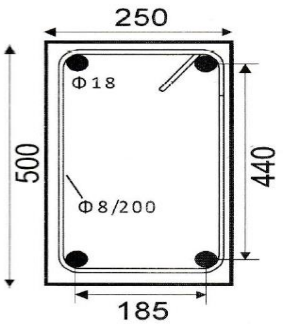

Figure 1. Cross Section of the Experimental Columns

Specimen	U_0S	C_0S	C_C2Sin	C_C2S	C_C5S	C_G5S
f_c (MPa)	18.3	18.3	18.1	18.1	20.4	18.7
N (kN)	190	182	167	190	182	182
v	0.38	0.38	0.37	0.38	0.34	0.37
Retrofitting Material	-	-	CFRP	CFRP	CFRP	GFRP
Retrofitting Layers	0	0	2	2	5	5
Loading Axis	strong	strong	strong	strong	strong	strong
Preloading	no	no	yes	no	no	no
δ_u (mm)	40.41	45.76	72.75	80.16	61.48	69.39
δ_y (mm)	14.66	11.50	23.25	12.70	9.29	8.40

Table 1. Compressive strength, maximum axial force and normalized axial force of the specimens

In the above table, the first letter of each specimen indicates whether the steel was corroded (C) or not corroded (U), the second and third letters indicate the retrofit material of the jacket (C for CFRP and G for GFRP) and the number of layers, respectively, S indicates that the specimens were tested through their strong axis, while the term "in" indicates that the specimen had been damaged through previous cyclic loading. N is the axial load, δ_u is the ultimate displacement, and δ_y is the displacement at yield.

3.2 Results and comparisons with the experimental data

The data referred to in the above section was applied to calculate the chord rotation ductility index. The results are shown in detail in Tables 2 and 3.

Specimen	Experimental	Approx. KAN.EPE. eq. (1)	Approx. KAN.EPE. eq. (2)	EC8-3 eq. (7)	Alternative EC8-3 eq. (14)
U_0S	2.76	1.63	1.96	3.56	2.35
C_0S	3.98	1.63	1.95	4.06	2.68

Table 2. Chord rotation ductility index of the unstrengthened specimens

Specimen	Experimental	Approx. KAN.-EPE. eq. (1)	Approx. KAN.-EPE. eq. (2)	EC8-3 eq. (7)	Alterative EC8-3 eq. (16)	Alterative EC8-3 eq. (17)	Alterative EC8-3 eq. (18)
C_C2Sin	3.13	1.90	2.35	3.55	3.10	5.67	4.74
C_C2S	3.13	1.87	2.30	5.65	3.35	5.60	4.68
C_C5S	6.62	2.88	3.82	6.84	4.24	5.77	4.53
C_G5S	8.26	7.97	11.5	6.24	3.78	5.80	4.47

Table 3. Chord rotation ductility index of the strengthened specimens

From the above results, it is evident that divergences exist between the experimental results and those of the models. The approximate equations of KAN.EPE. [1] give more conservative results, with the exception of the GFRP retrofitted column where equation (1) closely approaches the index μ_θ of the experimental result, whereas equation (2) exceeds it. On the other

hand, the values from equation (7) of EC8-3 [2] are in excess of the experimental value for the GFRP 5 layer specimen. Concerning the alternative equations to EC8-3 [2] presented by Fardis [3], equation (16), (17), and (18) give more conservative results to those of equation (7). Equation (16) gives similar results to the experimental for the 2 layer specimens. Equation (16) is the most conservative, while equation (17) is the least conservative. Note that for the specimens with corroded steel, increasing the FRP layer thickness increases the ductility, which indicates retrofitting with FRP can offset the detrimental effect of corroded steel.

3.3 Comparison between the models

For better understanding of the models, a comparison was made between different values of normalized axial force and nominal thickness of the FRP as well as between a constant value normalized axial force and increasing thickness of CFRP and GFRP.

Figure 2 compares the various models when determining the chord rotation ductility index for different values of normalized axial force. For this comparison, 5 layers of CFRP were used with $t_f = 0.13$ mm, $E_f = 230$ GPa, $f_u = 3450$ MPa and $\varepsilon_{ju} = 0.015$.

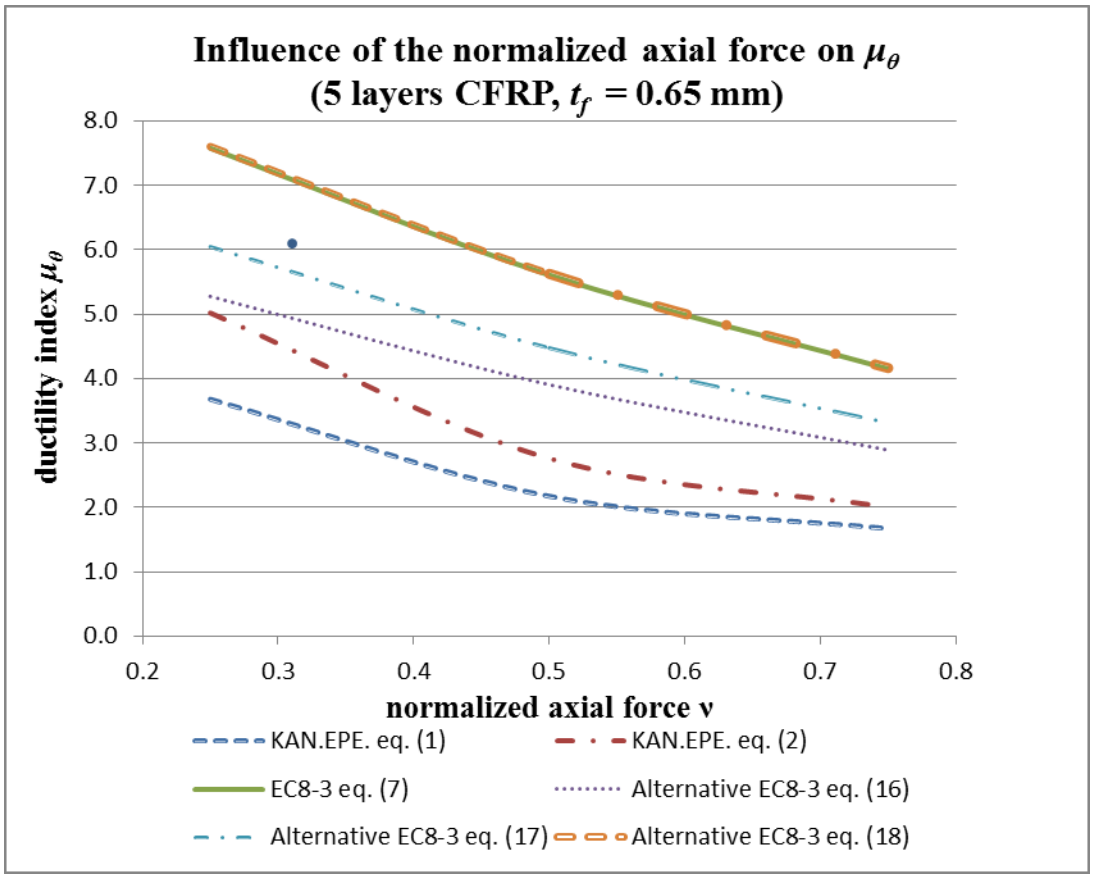

Figure 2. Influence of Normalized Axial Force on μ_θ

Figure 2 shows that all models are affected by changing the normalized axial force. The influence of the reduced axial force to the approximate models of KAN.EPE. [1] was expected, as the curvature ductility index is inversely proportional to the normalized axial force. The influence of the normalized axial force on the other models can be attributed to the term 0.3^{ν} that is in the equation for all EC8-3 [2] and Fardis [3] models. Indeed, for a range of normalized axial force from 0.25 to 0.80, this term gives values from 0.74 to 0.38, which causes the divergence in the results as the CFRP layer thickness is constant. This is unrealistic as the

models should only be affected by the change in the thickness of the FRP layers and not by the term v.

The convergence of the results between EC8-3 equation (7) model and the alternative model of Fardis [3] equation (18) is worth noting, as the results of the ductility index of those two models differ only in the second decimal place.

Finally, the dot in figure 2 represents the ductility index derived from the experimental data for specimen C_C5S and it can be seen that the best convergence between the experimental result and the analytical models is given by equation (17) of Fadis [3].

Figure 3 presents the effect of changing the CFRP layer thickness on the chord rotation ductility index for a constant value of normalized axial force equal to 0.5. For this comparison, E_f = 230 GPa, f_u = 3450 MPa, and ε_{ju} = 0.015.

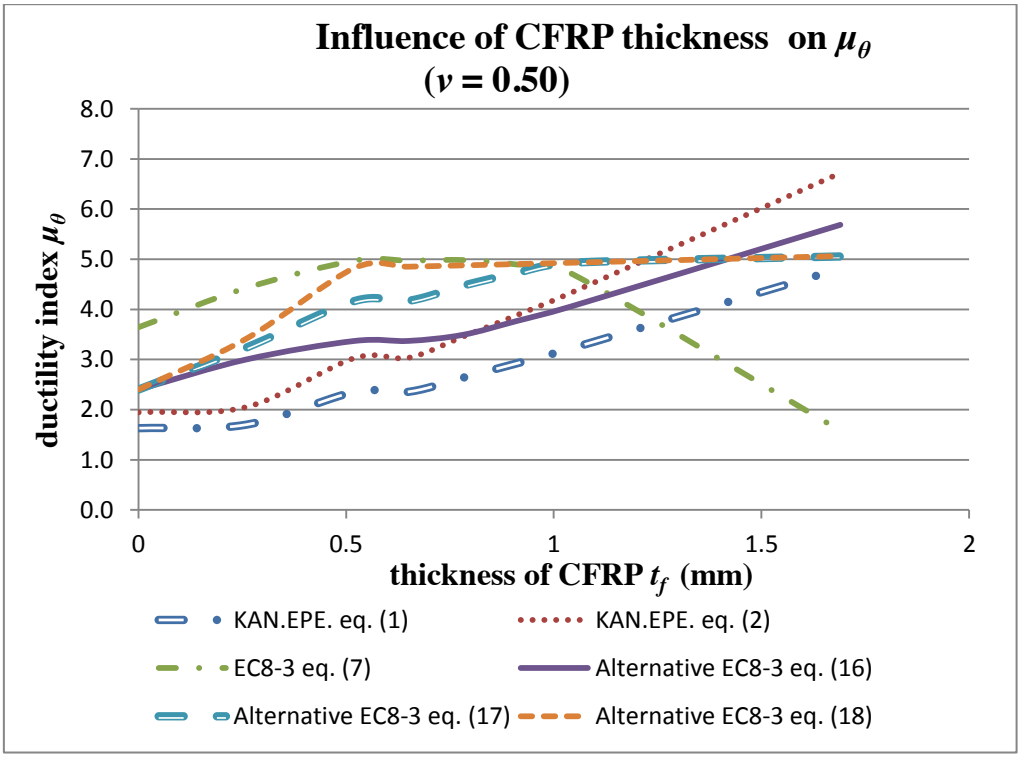

Figure 3. Influence on Ductility Index of Increasing CFRP Layer Thickness with Constant Normalized Axial Force

Figure 3 clearly shows that equation (7) of EC8-3 [2] initially has an upward trend, then stabilizes and finally trends downwards at 1 mm thickness of CFRP, which is illogical. The alternative models of EC8-3 [2] of Fardis [3] (equations (16), (17) and (18)) give markedly improved ductility index values in comparison to the basic model (equation (7)). It can be seen that equations (17) and (18) reach a certain thickness value and then give constant values for increased thicknesses. This indicates a limit to the increase in the ductility as the CFRP layers increase.

3.4 Influence of the different types of strengthening material on ductility

Figure 4 presents a comparison of the influence of the type of strengthening material on the calculation of the chord rotation ductility index. For CFRP, t_f = 0.13 mm, E_f = 230 GPa, f_u = 3450 MPa, and ε_{ju} = 0.015, while for GFRP, t_f = 0.17 mm, E_f = 70 GPa, f_u = 2170 MPa, and ε_{ju} = 0.031. The normalized axial force was constant and equal to 0.5.

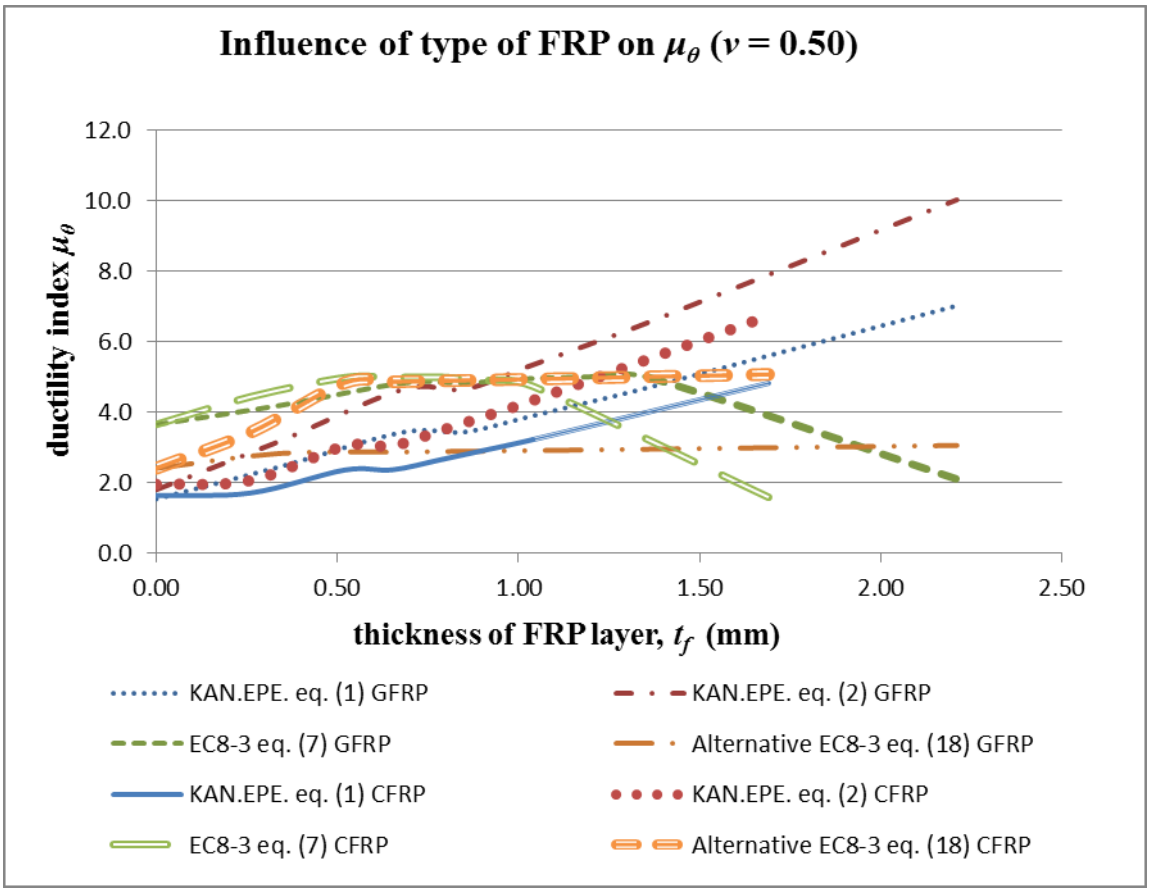

Figure 4. Influence of FRP Type on the Ductility Index for a Constant Normalized Axial Force

Figure 4 clearly shows that the type of FRP material affects the ductility index values. The basic model of EC8-3 [2] is an exception to this, as it is not particularly affected by the type FRP. The approximate models of KAN.EPE. [1] present a slight deviation of the ductility index between them for the same material layer thickness, with the values for GFRP being greater than those for CFRP. It is to be noted the deviation of the μ_θ values that derive from the alternative model of EC8-3 [2] of Fardis [3] (equation (18)). This deviation is due to the factor c_f , which was 1.8 for CFRP and 0.8 for GFRP. In fact, it is the only model in which the values of μ_θ for CFRP are greater than those of GFRP.

4 CONCLUSIONS

- The increase in the ductility index is feasible in columns with corroded reinforcement. This fact is attributed to the increase in deformability of the confined concrete inhibiting the buckling of longitudinal reinforcement and limiting shear.
- All ductility index calculation models were affected by a change in the normalized axial force. The influence of the normalized axial force on the approximate models of KAN.EPE. [1] was due to the curvature ductility index being inversely proportional to the normalized axial force. The influence of the normalized axial force on the basic Eurocode 8-3 [2] model and the Fardis [3] alternative models was attributed to the term 0.3^{v}, where v is the normalized axial force. Further research into this term would be wise, as the models should only be affected by the change in the thickness of the retrofitting layers and not by the term normalized axial force.

- The basic Eurocode 8-3 [2] model used to calculate the chord rotation ductility index acquires unrealistic values for large thicknesses of fiber reinforced polymer. The alternative models proposed by Fardis [3] improve this situation. However, two of the alternative models gave an upper limit to the increase of chord rotation ductility for increased fiber reinforced polymer layer thickness.
- All the models used to calculate the chord rotation ductility index show a slight influence depending on the type of reinforcement material used (carbon fiber reinforced polymer or glass fiber reinforced polymer) with the exception of the basic model of Eurocode 8-3 [2].
- Finally, the term c_f in one of the alternative Eurocode 8-3 [2] models proposed by Fardis [3], should be further investigated as it greatly affects the chord rotation ductility index depending on the type of fiber reinforced polymer used.

REFERENCES

[1] KAN.EPE., *Greek code for structural interventions*. Earthquake Planning and Protection Organization, Greek Ministry for Environmental Planning and Public Works, Athens, Greece, 2013 and draft 2017.

[2] EC8-3, *Eurocode 8 part 3, Design of structures for earthquake resistance: Assessment and retrofitting of buildings*. EN 1998-3: European Committee for Standardization, CEN/TC250, Brussels, 2005.

[3] M.N. Fardis, *Seismic design, assessment and retrofitting of concrete buildings based on EN-Eurocode 8,* Dordrecht, Springer Science+Business Media B.V., 2009.

[4] S.N. Bousias, T.C. Triantafillou, M.N. Fardis, L. Spathis, and B.A. O'Regan, Fiber-reinforced polymer retrofitting of rectangular reinforced concrete columns with or without corrosion. *ACI Structural Journal*, **101(4)**, 512-520, 2004.